COMPUTATION OF TURBULENT FREE-SURFACE FLOWS USING $\kappa - \varepsilon$ MODELS

V. G. Ferreira
Departamento de Estatística, Matemática Aplicada e Computação, Instituto de Geociências e Ciências Exatas Av. 24-A, 1515 - C.P. 178 - 13500-230, Rio Claro, SP, Brazil
e-mail, pvgf@lcad.icmc.sc.usp.br

J. A. Cuminato
Departamento de Ciências de Computação e Estatística, Instituto de Ciências Matemáticas e de Computação Av. Trabalhador São Carlense, 400, C.P. 668, 13251-900, São Carlos, SP, Brazil
e-mail, jacumina@lcad.icmc.sc.usp.br

N. Mangiavacchi
Departamento de Ciências de Computação e Estatística, Instituto de Ciências Matemáticas e de Computação Av. Trabalhador São Carlense, 400, C.P. 668, 13251-900, São Carlos, SP, Brazil
e-mail, norberto@lcad.icmc.sc.usp.br

M. F. Tomé
Departamento de Ciências de Computação e Estatística, Instituto de Ciências Matemáticas e de Computação Av. Trabalhador São Carlense, 400, C.P. 668, 13251-900, São Carlos, SP, Brazil
e-mail, murilo@lcad.icmc.sc.usp.br

A. Castelo Filho
Departamento de Ciências de Computação e Estatística, Instituto de Ciências Matemáticas e de Computação Av. Trabalhador São Carlense, 400, C.P. 668, 13251-900, São Carlos, SP, Brazil
e-mail, castelo@lcad.icmc.sc.usp.br

S. McKee
Department of Mathematics, University of Strathclyde, Livingstone Tower 26 Richmond Street, Glasgow, G1 1XH, Scotland, UK
e-mail, caas29@maths.strath.ac.uk

Abstract. *This paper presents numerical simulations of incompressible turbulent free-surface fluid flow problems. The methodology employed to solve the time-averaged Navier-Stokes, mass conservation and $\kappa - \varepsilon$ turbulence equations is an extension of GENSMAC: a finite-difference marker-and-cell technique for the numerical solution of incompressible free-surface flows using a velocity-pressure formulation. The numerical solution procedure is applied to a turbulent boundary-layer on a flat plate and an axisymmetric jet impinging onto a flat surface.*

Keywords: *turbulent flow; time-averaged Navier-Stokes; free-surface fluid flow; high-order upwinding; finite-difference formulation; $\kappa - \varepsilon$ turbulence model*

1. Introduction

Numerical solutions of the time-averaged Navier-Stokes equations for turbulent flow field have received a great deal of attention in recent years, since, in principle, they describe fluid flow problems with any level of complexity. The only uncertanty in this approach is that introduced by turbulence model to effect closure of the mean conservation equations. The effects of the turbulence in the fluid flow sometimes play an important part in the physical process because of its increased mixing properties, which can affect the overall temperature, density and velocity distributions in the flow. However, compared to confined fluid flow problems, the numerical solution of turbulent free-surface fluid flow problems represents a challenge, since the free-surface itself is one of the unknowns.

The main purpose of this work is to present numerical simulations of incompressible turbulent free-surface fluid flow problems using two versions of the $\kappa - \varepsilon$ turbulence model. The numerical solution procedure is applied to a turbulent boundary-layer on a flat plate and an axisymmetric jet impinging onto a flat surface.

2. Governing Equations

The set of governing equations for time-dependent, viscous, isothermal incompressible turbulent newtonian fluid flow are the time-averaged Navier-Stokes equations, mass conservation equation, and κ and ε equations. In conservative form, these fluid flow equations, omitting averaging symbols, can be written as, respectively,

$$\frac{\partial u}{\partial t}+\frac{1}{r^\alpha}\frac{\partial (r^\alpha uu)}{\partial r}+\frac{\partial (uv)}{\partial z}=-\frac{\partial p_e}{\partial r}+\frac{1}{Re}\frac{\partial}{\partial z}\left(\frac{\partial u}{\partial z}-\frac{\partial v}{\partial r}\right)+\frac{1}{Fr^2}g_r$$

$$+\quad \frac{1}{Re}\left[2\frac{1}{r^\alpha}\frac{\partial}{\partial r}\left(r^\alpha \nu_t \frac{\partial u}{\partial r}\right)+\frac{\partial}{\partial z}\left(\nu_t\left(\frac{\partial u}{\partial z}+\frac{\partial v}{\partial r}\right)\right)-2\alpha\frac{\nu_t u}{r^{2\alpha}}\right], \tag{1}$$

$$\frac{\partial v}{\partial t}+\frac{1}{r^\alpha}\frac{\partial (r^\alpha vu)}{\partial r}+\frac{\partial (vv)}{\partial z}=-\frac{\partial p_e}{\partial z}-\frac{1}{Re}\frac{1}{r^\alpha}\frac{\partial}{\partial r}\left(r^\alpha\left(\frac{\partial u}{\partial z}-\frac{\partial v}{\partial r}\right)\right)+\frac{1}{Fr^2}g_z$$

$$+\quad \frac{1}{Re}\left[2\frac{\partial}{\partial z}\left(\nu_t\frac{\partial v}{\partial z}\right)+\frac{1}{r^\alpha}\frac{\partial}{\partial r}\left(r^\alpha\nu_t\left(\frac{\partial u}{\partial z}+\frac{\partial v}{\partial r}\right)\right)\right], \tag{2}$$

$$\frac{1}{r^\alpha}\frac{\partial (r^\alpha u)}{\partial r}+\frac{\partial v}{\partial z}=0, \tag{3}$$

$$\frac{\partial \kappa}{\partial t}+\frac{1}{r^\alpha}\frac{\partial (r^\alpha u\kappa)}{\partial r}+\frac{\partial (v\kappa)}{\partial z}=\frac{1}{Re}\left[\frac{1}{r^\alpha}\frac{\partial}{\partial r}\left(r^\alpha(1+\nu_t/\sigma_\kappa)\frac{\partial \kappa}{\partial r}\right)+\frac{\partial}{\partial z}\left((1+\nu_t/\sigma_\kappa)\frac{\partial \kappa}{\partial z}\right)\right]+P-\varepsilon, \tag{4}$$

$$\frac{\partial \varepsilon}{\partial t}+\frac{1}{r^\alpha}\frac{\partial (r^\alpha u\varepsilon)}{\partial r}+\frac{\partial (v\varepsilon)}{\partial z}=\frac{1}{Re}\left[\frac{1}{r^\alpha}\frac{\partial}{\partial r}\left(r^\alpha(1+\nu_t/\sigma_\varepsilon)\frac{\partial \varepsilon}{\partial r}\right)+\frac{\partial}{\partial z}\left((1+\nu_t/\sigma_\varepsilon)\frac{\partial \varepsilon}{\partial z}\right)\right]$$

$$+\quad (C_{1\varepsilon}P-C_{2\varepsilon}\varepsilon)/T_t+\beta E. \tag{5}$$

In the above equations, t is the time, $u=u(r,z,t)$ and $v=v(r,z,t)$ are, respectively, the components in the r and z directions of the local time-averaged velocity vector field $\mathbf{u}=\mathbf{u}(r,z,t)$, $\kappa=\kappa(r,z,t)$ is the time-averaged turbulent kinetic energy, $\varepsilon=\varepsilon(r,z,t)$ is the dissipation rate of κ, and $p_e=p+\frac{2}{3}\frac{1}{Re}\kappa$ is the effective pressure. The non-dimensional parameters $Re=U_0L_0/\nu$ and $Fr=U_0/\sqrt{L_0|\mathbf{g}|}$ denote the associated Reynolds and Froude numbers, respectively, in which U_0 is a characteristic velocity scale, L_0 is a length scale, and ν is the kinematic viscosity of the fluid. The isotropic eddy-viscosity ν_t, the production of turbulence P, the source term E and the time scale T_t are, respectively, defined as

$$\nu_t=C_\mu f_\mu \kappa T_t, \tag{6}$$

$$P=\nu_t\left(2\left(\frac{\partial u}{\partial r}\right)^2+2\left(\frac{\partial v}{\partial z}\right)^2+2\alpha\left(\frac{u}{r^\alpha}\right)^2+\left(\frac{\partial v}{\partial r}+\frac{\partial u}{\partial z}\right)^2\right), \tag{7}$$

$$E=\frac{2\nu_t}{Re}\left(\left(\frac{\partial^2 v}{\partial r^2}\right)^2+\left(\frac{\partial^2 u}{\partial z^2}\right)^2\right), \tag{8}$$

$$T_t=(1-\beta)Min\left\{\frac{\kappa}{\varepsilon},\frac{2}{3C_\mu}\sqrt{\frac{3}{8|\mathbf{S}|^2}}\right\}+\beta\left\{\frac{\kappa}{\varepsilon}+\left(\frac{1}{\varepsilon}\right)^{1/2}\right\}, \tag{9}$$

where, in Eq. (9), $|\mathbf{S}|^2=\mathbf{D}:\mathbf{D}$, with $\mathbf{D}=\nabla\mathbf{u}+(\nabla\mathbf{u})^{\mathbf{T}}$. Together with the model constants C_μ, $C_{1\varepsilon}$, $C_{2\varepsilon}$, σ_κ and σ_ε, the parameter β in Eqs. (5) and (9) is used to specify the $\kappa-\varepsilon$ models. In the case of $C_\mu=0.09$, $C_{1\varepsilon}=1.44$, $C_{2\varepsilon}=1.92$, $\sigma_\kappa=1.0$, $\sigma_\varepsilon=1.3$ and $\beta=0$, we deal with the high-Reynolds $\kappa-\varepsilon$ model of Lauder and Spalding, 1974 (HRe $\kappa-\varepsilon$ model), with the time scale proposed by Durbin, 1996 for appropriated treatment of stagnation-point anomaly. When the model constants are that proposed by Hoffman, 1975; that is, $C_\mu=0.09$, $C_{1\varepsilon}=1.81$, $C_{2\varepsilon}=2.0$, $\sigma_\kappa=2.0$, $\sigma_\varepsilon=3.0$ and $\beta=1$, we treat with a low-Reynolds $\kappa-\varepsilon$ model (LRe $\kappa-\varepsilon$ model), similar to that proposed by Yang and Shih, 1993. The damping function f_μ in Eq. (6) assumes the value $f_\mu=1$ in the case of the HRe $\kappa-\varepsilon$ model, and takes the following expression in the case of the LRe $\kappa-\varepsilon$ model

$$f_\mu=\left(1-Exp(-a_1Re_{z_w}-a_3Re_{z_w}^3-a_5Re_{z_w}^5)\right)^{1/2}, \tag{10}$$

where a_1, a_3 and a_5 are constants given by $a_1=1.5\times10^{-4}$, $a_3=5.0\times10^{-7}$, $a_5=1.0\times10^{-10}$, and Re_{z_w} is the local Reynolds number defined as $Re_{z_w}=z_wRe\kappa^{1/2}$, being z_w the normal distance from the rigid-boundary to a point into the flow. The parameter α in Eqs. (1) through (7) is used to specify the coordinate system, namely: when $\alpha=0$, plane cartesian coordinates is considered; and when $\alpha=1$, cilyndrical polar coodinates is assumed. The dependent variables in Eqs. (1)-(9) have been nondimensionalized by U_0, L_0 and ν in the usual way.

3. Initial and Boundary Conditions

Equations (1) through (5) are coupled, non-linear, partial differential equations and, together with the eddy-viscosity model (6), are sufficient, in principle, to solve for the five unknowns u, v, p_e, κ and ε when appropriated initial and boundary conditions are specified. In this work, a staggered grid is used where the effective pressure, the turbulent kinetic energy and the dissipation rate are stored at the center of a computational cell, whereas velocities are stored at the cell boundaries. With this grid system, effective pressure boundary conditions are not needed. For initial conditions, the values of all variables are prescribed. Five types of boundary conditions are used, namely: inflow, outflow, symmetry, free-surface, and rigid-wall boundaries. At the inflow, the values of u, v, κ and ε are prescribed. At the outflow, the streamwise gradient for each variable is required to be equal to zero. At symmetry boundaries, we are using

$$u_n = 0, \quad \frac{\partial u_t}{\partial n} = 0, \quad \frac{\partial \kappa}{\partial n} = 0 \quad \text{and} \quad \frac{\partial \varepsilon}{\partial n} = 0, \tag{11}$$

where n and t denote normal and tangential directions to the boundary, respectively. At the free-surface, we are considering that the fluid is moving into a passive atmosphere (zero-pressure) and, in the absence of surface tension forces, the normal and tangential components of the stress must be continuous across any free-surface, so that on such a surface we have (see, for example, Ladau and Lifshitz, 1987)

$$\mathbf{n} \cdot (\sigma \cdot \mathbf{n}) = 0, \tag{12}$$

$$\mathbf{m} \cdot (\sigma \cdot \mathbf{n}) = 0. \tag{13}$$

Here, $\mathbf{n}$ and $\mathbf{m}$ are unit normal and tangent vectors to the surface, and σ is the general constitutive equation (Cauchy stress-tensor) defined as

$$\sigma = -p_e \, \mathbf{I} + \frac{1}{Re}(1 + \nu_t)\mathbf{D}, \tag{14}$$

where $\mathbf{I}$ denotes the identity tensor. From Eqs. (12) and (13), we determine the effective pressure and the velocities, respectively. The turbulent variables at the free-surface are determined by imposing

$$\frac{\partial \kappa}{\partial n} = 0 \quad \text{and} \quad \frac{\partial \varepsilon}{\partial n} = 0. \tag{15}$$

The boundary conditions at rigid-wall depend on the $\kappa - \varepsilon$ model considered. When the simulation is performed with the HRe $\kappa - \varepsilon$ model, the wall-function approach of Lauder and Spalding, 1974 is used. In this case, the fundamental equation for determining the fictitious velocities and turbulent variables near a rigid-wall is the total wall shear stress τ_w given by (Wilcox, 1988)

$$\frac{1}{Re}(1 + \nu_t)\left|\frac{\partial \hat{u}}{\partial n}\right| \approx {u_\tau}^2 = \tau_w, \tag{16}$$

where $\hat{u}$ represents the velocity component tangential to the rigid-wall, and u_τ is the friction velocity. The values of the κ and ε in the inertial sublayer are given by

$$\kappa = Re\frac{\tau_w}{C_\mu^{1/2}} \quad \text{and} \quad \varepsilon = Re\frac{\tau_w u_\tau}{K z_w}, \tag{17}$$

being $K = 0.41$ the von Kármán constant. In the viscous sublayer, we are using the strategy of Sondak and Pletcher, 1995, that is,

$$\kappa = Re\frac{\tau_w}{C_\mu^{1/2}}\left(\frac{z^+}{{z_c}^+}\right)^2 \quad \text{and} \quad \varepsilon = \sqrt{\frac{1}{Re}}\frac{\kappa^{3/2}}{l^*}, \tag{18}$$

where z^+ is defined as $z^+ = Re u_\tau z_w$ and l^* represents the length scale proposed by Norris and Reynolds, 1975. Neglecting the buffer layer of a turbulent boundary-layer, the critic z^+ (${z_c}^+$) in Eq. (18) delimits the viscous sublayer and the inertial sublayer. A detailed discussion of the initial and boundary conditions using the HRe $\kappa - \varepsilon$ turbulence model is given in Ferreira, 2001. When the LRe $\kappa - \varepsilon$ model is used in the simulations, the velocity at solid boundary is set to zero, in order to represent the no-slip condition ($\mathbf{u} = \mathbf{0}$), and the values of the variables κ and ε at this boundary are (Merci et al., 2001)

$$\kappa = 0 \quad \text{and} \quad \varepsilon = \frac{2}{Re}\left(\frac{\partial \kappa^{1/2}}{\partial n}\right)^2. \tag{19}$$

3.1. Wall-Function Application

It is well known that the $HRe\ \kappa - \varepsilon$ model requires modification for the simulation of flow near rigid boundaries, so as to account for damping of velocity flutuations and viscous effects. In general, the solution of the conservation equations in the inner layer is not necessary since the flow mechanism in such a region can be described reasonably well by employing wall-functions (for a more datailed discussion see, for example, Ferreira, 2001). The behavior of the mean velocity profiles in the viscous and inertial sublayers are, respectively, given by (see, for example, Bradshaw, 1976, Wilcox, 1988 or White, 1991)

$$u^+ - z^+ = 0, \tag{20}$$

$$ln(Ez^+) - Ku^+ = 0, \tag{21}$$

where $u^+ = \hat{u}/u_\tau$ and $E = exp(K5.1)$. One of the central questions in the application of the wall-functions (16)-(18) is the determination of the friction velocity, and hence the wall shear stress. It is determined from relation (20) or (21), depending on the local Reynolds number z^+. When u_τ is obtained by (21), Newton-Raphson's method is applied with $u_\tau = 11.60$ as the initial condition. We initiate the calculations by determining the critic Reynolds number ${z_c}^+$, solution of the non-linear equation defined by the intersection of (20) and (21), and by imposing that it is in the viscous sublayer. By neglecting the transition sublayer, in every cycle of the computational procedure, the friction velocity is estimated in the following manner: with the tangential velocity $\hat{u}$ known in the first cell adjacent to the wall, u_τ is apdated according to the value of the z^+ given by (20). If z^+ is less than ${z_c}^+$, we use (20); on the other hand, we employ (21). The fictitious velocities are calculated by central-difference approximation of the Eq. (16).

4. Numerical Methodology

The governing equations (1) through (5) are solved with an extension of the GENSMAC methodology for turbulent flow field (see Ferreira, 2001). It is based on the decomposition of vector field into a divergence free component and a gradient of a scalar field. The detailed information of the GENSMAC for laminar flow field is provided by Tomé and McKee, 1994 and Tomé et al., 2000.

GENSMAC is a finite-difference, explicit, first/second-order accurate numerical method based on a predictor-corrector scheme. By using a guessed effective pressure $\tilde{p}_e$ and an eddy-viscosity, the method consists of solving the time-averaged Navier-Stokes equations at the $(k+1)$ time-step for a tentative velocity field $\tilde{\mathbf{u}}$. The $\tilde{\mathbf{u}}$ is related to the true velocity field $\mathbf{u}$, at the $(k+1)$ time-step, by an auxiliary potential function ψ which is calculated by a Poisson equation, originated by imposing $\nabla \cdot \mathbf{u} = 0$ at the $(k+1)$ time-step. The effective pressure and the turbulent variables κ and ε are then updated, and the procedure is repeated at each time-step. In particular, when calculating $\tilde{\mathbf{u}}$ in step 1, we employ an adaptive time-stepping routine (see Tomé and McKee, 1994). The numerical solution procedure may be summarized as follows.

It is supposed that, at a given time $t = t_0$, the velocity field $\mathbf{u}$ is known and suitable boundary conditions for the velocity and turbulent variables are given. Let $\tilde{p}_e(r,z,t)$ be an arbitrary effective pressure field, which satisfies the correct pressure condition on the free-surface. This pressure field is constructed employing the normal-stress condition (12) at the free-surface, and it is chosen arbitrarily (for instance $\tilde{p}_e(r,z,t) = 0$) into the fluid. The updated velocity field, the effective pressure and the turbulent variables, at time $t = t_0 + \delta t$, are calculated by the following steps:

1. With the eddy-viscosity ν_t known at $t = t_0$, compute an approximate velocity field $\tilde{\mathbf{u}}(r,z,t)$ from a finite-difference discretization of

$$\left.\frac{\partial \tilde{u}}{\partial t}\right|_{t=t_0} = \left\{ -\frac{1}{r^\alpha}\frac{\partial (r^\alpha uu)}{\partial r} - \frac{\partial (uv)}{\partial z} - \frac{\partial \tilde{p}_e}{\partial r} + \frac{1}{Re}\frac{\partial}{\partial z}\left(\frac{\partial u}{\partial z} - \frac{\partial v}{\partial r}\right) + \frac{1}{Fr^2}g_r \right.$$

$$\left. + \frac{1}{Re}\left[2\frac{1}{r^\alpha}\frac{\partial}{\partial r}\left(r^\alpha \nu_t \frac{\partial u}{\partial r}\right) + \frac{\partial}{\partial z}\left(\nu_t\left(\frac{\partial u}{\partial z} + \frac{\partial v}{\partial r}\right)\right) - 2\alpha\frac{\nu_t u}{r^{2\alpha}}\right] \right\}\Bigg|_{t=t_0}, \tag{22}$$

$$\left.\frac{\partial \tilde{v}}{\partial t}\right|_{t=t_0} = \left\{ -\frac{1}{r^\alpha}\frac{\partial (r^\alpha vu)}{\partial r} - \frac{\partial (vv)}{\partial z} - \frac{\partial \tilde{p}_e}{\partial z} - \frac{1}{Re}\frac{1}{r^\alpha}\frac{\partial}{\partial r}\left(r^\alpha\left(\frac{\partial u}{\partial z} - \frac{\partial v}{\partial r}\right)\right) + \frac{1}{Fr^2}g_z \right.$$

$$\left. + \frac{1}{Re}\left[2\frac{\partial}{\partial z}\left(\nu_t\frac{\partial v}{\partial z}\right) + \frac{1}{r^\alpha}\frac{\partial}{\partial r}\left(r^\alpha \nu_t\left(\frac{\partial u}{\partial z} + \frac{\partial v}{\partial r}\right)\right)\right] \right\}\Bigg|_{t=t_0}, \tag{23}$$

with $\widetilde{\mathbf{u}}(r,z,t_0) = \mathbf{u}(r,z,t_0)$ using the correct boundary conditions for $\mathbf{u}(r,z,t_0)$. It can be shown (see, for example, Ferreira, 2001) that $\widetilde{\mathbf{u}}(r,z,t)$ possesses the correct vorticity at time t but does not satisfy (3), in general. By writting

$$\mathbf{u}(r,z,t) = \widetilde{\mathbf{u}}(r,z,t) - \nabla\psi(r,z,t) \tag{24}$$

and imposing

$$\nabla^2\psi(r,z,t) = \nabla\cdot\widetilde{\mathbf{u}}(r,z,t), \tag{25}$$

a velocity field is obtained in which the vorticity and mass are conserved;

2. Solve the Poisson equation (25). The appropriate boundary conditions for this elliptic equation are homogeneous Dirichlet-type on the free-surface and homogeneous Neumann-type on fixed boundaries. These are treated in a similar way as is in the GENSMAC code of Tomé and McKee, 1994;

3. Calculate the velocity field $\mathbf{u}(r,z,t)$ from (24);

4. Compute the effective pressure. It can be shown (see Ferreira, 2001) that the effective pressure field is given by

$$p_e(r,z,t) = \tilde{p}_e(r,z,t) + \psi(r,z,t)/\delta t; \tag{26}$$

5. Compute the kinetic energy κ from a finite-difference approximation of (4);

6. Compute the dissipation rate ε from a finite-difference approximation of (5);

7. Update the eddy-viscosity ν_t from (6);

8. Particle movement. The last step in the calculation involves the movement of the marker particles to their new positions. These are virtual particles (without mass, volume, or other properties), whose coordinates are stored and updated at the end of each cycle by solving the ordinary differential equations

$$\frac{dr}{dt} = u \quad \text{and} \quad \frac{dz}{dt} = v \tag{27}$$

by Euler's method. This provides a particle with its new coordinates, allowing us to determine whether or not it has moved into a new computational cell, or if it has left the containment region through an outflow-boundary;

9. Update the boundary conditions and go back to the first step.

In the solution procedure outlined above, the differential equations are discretized in time and space in precisely the same manner for all dependent variables. The temporal derivatives are discretized using the first-order forward difference (Euler's method), while the spatial derivatives are evaluated using specific finite-differences on a uniform staggered grid system. The convective terms are approximated by the high-order upwinding VONOS scheme of Varonos and Bergeles, 1998, which satisfy the monotonicity criterion proposed by Gaskell and Lau, 1988. A detailed discussion of this convection scheme would go beyond the scope of this paper, and the reader is referred to Ferreira et al., 2002 for details of implementation and application. All the other derivatives are approximated using standard second-order central-difference formulation. The Poisson equation (25) is discretized using the usual five-point Laplacian operator, and the corresponding symmetric-positive definite linear system is solved by the conjugate-gradient method

5. Numerical Results and Discussions

First, results with the *HRe* $\kappa-\varepsilon$ model will be presented for the turbulent boundary-layer on a flat plate. For this problem, the Reynolds number based on the inflow velocity $U_0 = 1.0$ m/s and the channel height $H = 1.0$ m is $Re = 2.0\times10^6$. Three different meshes are used: a coarse mesh (20×100 computational cells, $\delta x = \delta y = 0.05$ m); a medium mesh (40×200 computational cells, $\delta x = \delta y = 0.025$ m); and a fine mesh (80×400 computational cells, $\delta x = \delta y = 0.0125$ m). Figure 1 shows a comparison between the dimensionless turbulent skin-friction coefficient profiles $C_f = 2\tau_w$, as a function of the local Reynols number $Re_x = U_0 x/\nu$, obtained by the *HRe* $\kappa-\varepsilon$ model, in the three meshes and at the adimensional time $t = 6.477$, and the estimates given

by Prandtl, power-law and White (see, for example, White, 1991). In this picture, for simple comparison, the laminar profile is also presented. As shown in Figs. 1 a), b) and c), the numerical estimates are generally satisfactory for Re_x beyond 1.0×10^6. It can also be observed from Fig. 1 d) that when the coarse mesh is twice refined, there was convergence of the numerical solution for a profile near the power-law and White profiles. On the other hand, for $Re_x \leq 1.0 \times 10^6$, the discrepancy may be due to the uniform meshes used and the initial velocity profile not being sufficiently turbulent at the entrance region. Of course, near to $Re_x = 1.0 \times 10^6$, it may be noticed the tendency of the numerical profile, in the fine mesh (Fig. 1 c)), to follow the theoretical profiles.

Next, results with both the $HRe\ \kappa - \varepsilon$ and $LRe\ \kappa - \varepsilon$ models will be examined for an axisymmetric jet impinging onto a flat surface. For this problem, the Reynolds number based on the inflow velocity $U_0 = 1.0$ m/s and inflow diameter $D = 0.02$ m is $Re = 5.03 \times 10^4$, and the Froude number is $F_r = U_0/\sqrt{gD}$. Three different meshes are also used for this free-surface flow: a coarse mesh (50×100 computational cells, $\delta r = \delta z = 0.001$ m); a medium mesh (100×200 computational cells, $\delta r = \delta z = 0.0005$ m); and a fine mesh (200×400 computational cells, $\delta r = \delta z = 0.00025$ m). Figure 2 shows a comparison between the dimensionless surface height h, obtained from the $HRe\ \kappa - \varepsilon$ (Figs. 2 a), c) and e) - left column) and $LRe\ \kappa - \varepsilon$ (Figs. 2 b), d) and f) - right column) models in the three meshes and at the adimensional time $t = 20.48$, and approximate viscous and inviscid solutions by Watson, 1964. It can be seen, from the left column of this figure, that the numerical solutions using the $HRe\ \kappa - \varepsilon$ model on coarse and medium meshes monotonicaly converge to the numerical solution on the fine mesh, and the numerical solution on the fine mesh shows reasonable agreement with the Watson's viscous solution. At the same adimensional time of the simulation with the $HRe\ \kappa - \varepsilon$ model, the comparison between the surface height obtained from the $LRe\ \kappa - \varepsilon$ model and the Watson's viscous solution was also made, and the results are displayed in the right column of the Fig. 2. It is clear that the numerical results with this turbulence model on coarse and medium meshes are unsatisfactory, whereas the solution on the fine mesh converges to a solution near Watson's viscous solution. We believe that, for this especific free-surface fluid flow problem, the discrepancy between viscous analytical solution, developed by Watson, and the numerical solution, obtained by the two versions of $\kappa - \varepsilon$ models, may be atributed to the poor resolution of the viscous sublayer by numerical methods and the hypotheses made by Watson to obtain his viscous analytical solutions. In fact, the numerical solutions have been calculated on uniform meshes; and the viscous analytical solution, according to Watson, is in disagreement with experimental data.

6. Summary and Conclusion

Numerical simulations of turbulent free-surface fluid flow problems by using two versions of the $\kappa - \varepsilon$ turbulent models have been presented. In order to describe the turbulent effects on the averaged flow, the κ and ε conservation equations were analysed and implemented into the two-dimensional and axisymmetric GENSMAC codes. In an attempt to obtain bounded transient solutions, the convection VONOS scheme was adopted for all non-linear derivatives of the convective transport equations. The numerical results show that it is beneficial to incorporate this high-order upwinding method in order to reduce the effects of numerical diffusion in turbulent free-surface flow problems. Particularly, on fine meshes, both the $\kappa - \varepsilon$ models yield favorable predictions of turbulent boundary-layer on a flat plate and jet impingement flows.

At the present, the authors are looking at the adaptation of these numerical techniques to more difficult fluid flow problems, such as those involving three dimensions.

7. Acknowledgments

This study has been supported by FAPESP and DEMAC/IGCE/UNESP.

8. References

Bradshaw, P., 1976, "Turbulence", Ed. Springer-Verlag, Germany, Topics in Applied Physics V. 12.

Durbin, P. A., 1996, On the $\kappa - \varepsilon$ Stagnation Point Anomaly, "Journal of Heat and Fluid Flow", Vol. 17, pp. 89–90.

Ferreira, V. G., 2001, "Análise e Implementação de Esquemas de Convecção e Modelos de Turbulência para Simulação de Escoamentos Incompressíveis Envolvendo Superfícies Livres", PhD thesis, ICMC-USP, São Carlos, Brazil.

Ferreira, V. G., Tomé, M. F., Mangiavacchi, N., Castelo, A., Cuminato, J. A., Fortuna, A. O., and McKee, S., 2002, High Order Upwinding and the Hydraulic Jump, "International Journal for Numerical Methods in Fluids", Vol. 39, *in press.*

Gaskell, P. H. and Lau, A. K. C., 1988, Curvature-Compensated Convective Transport: SMART, A New Boundedness-Preserving Transport Algorithm, "International Journal for Numerical Methods in Fluids", Vol. 8, pp. 617–641.

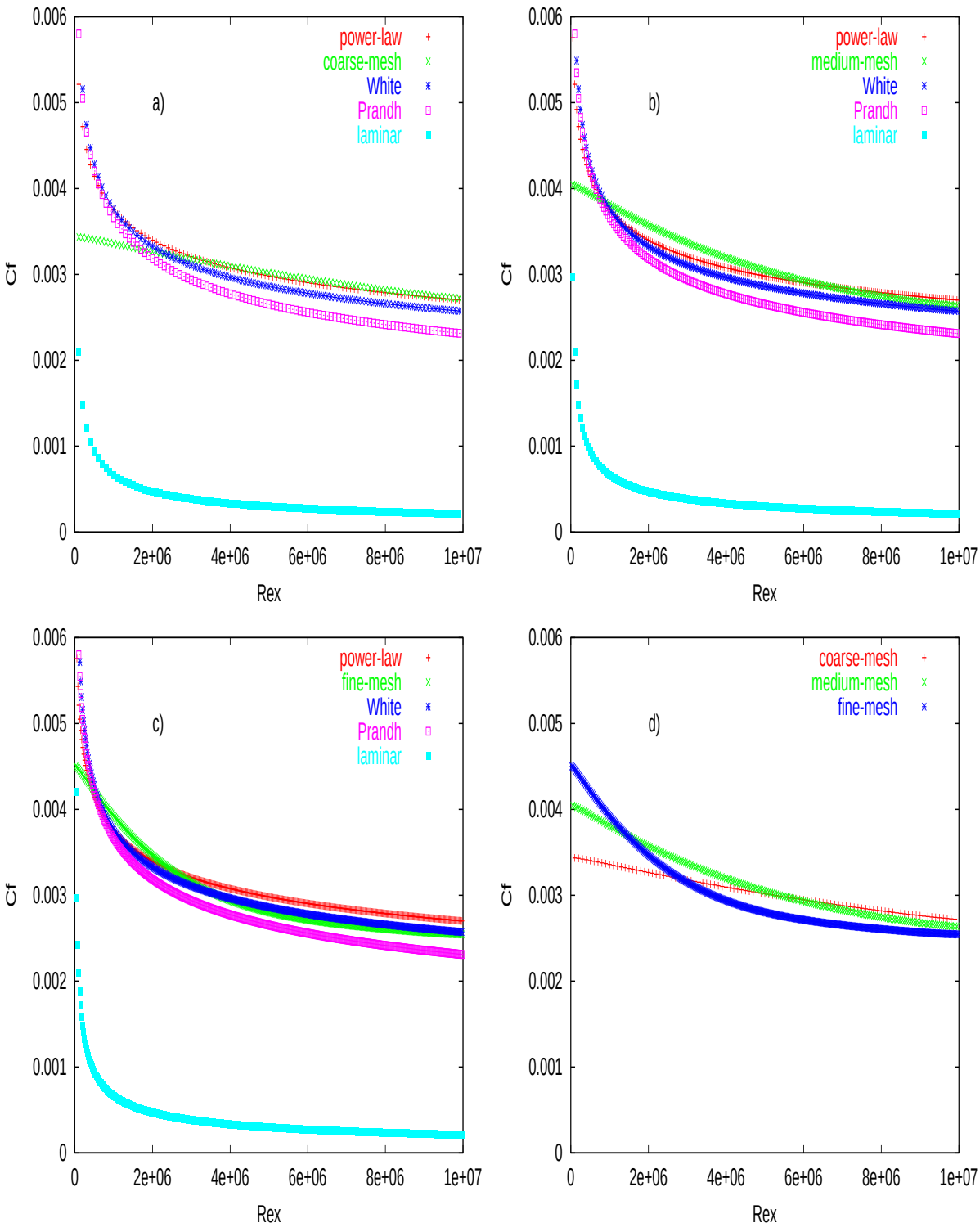

Figure 1: Comparison between the skin-friction coefficient profiles $C_f = C_f(Re_x)$ for the turbulent boundary-layer on a flat plate, showing theoretical estimates and that by HRe $\kappa - \varepsilon$ model: a) Comparison in the coarse mesh; b) Comparison in the medium mesh; c) Comparison in the fine mesh; d) Comparison of the three numerical solutions.

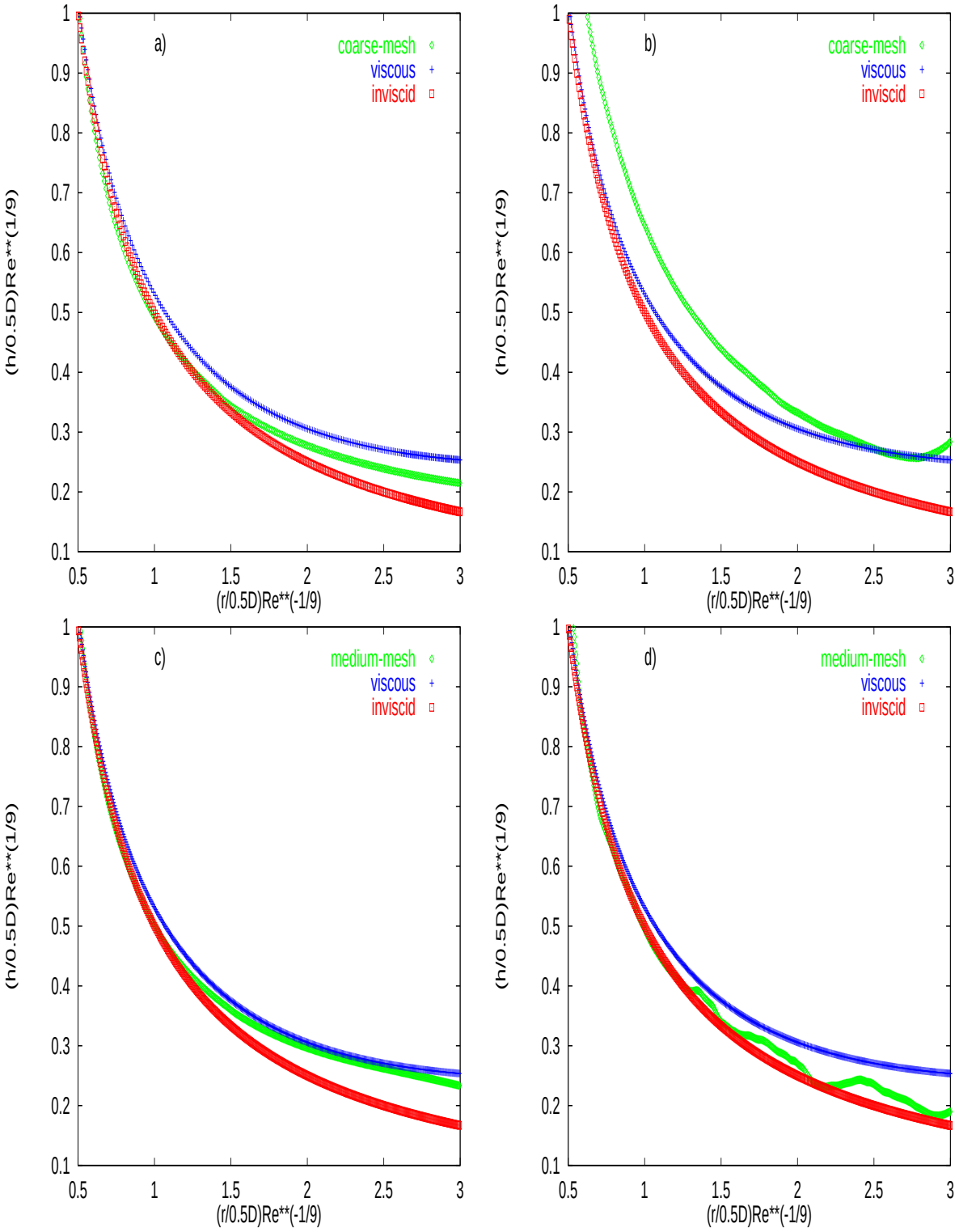

Figure 2: Comparison between the numerical solutions by using the $HRe\ \kappa-\varepsilon$ (left column) and $LRe\ \kappa-\varepsilon$ (right column) models and approximate analytical solutions by Watson.

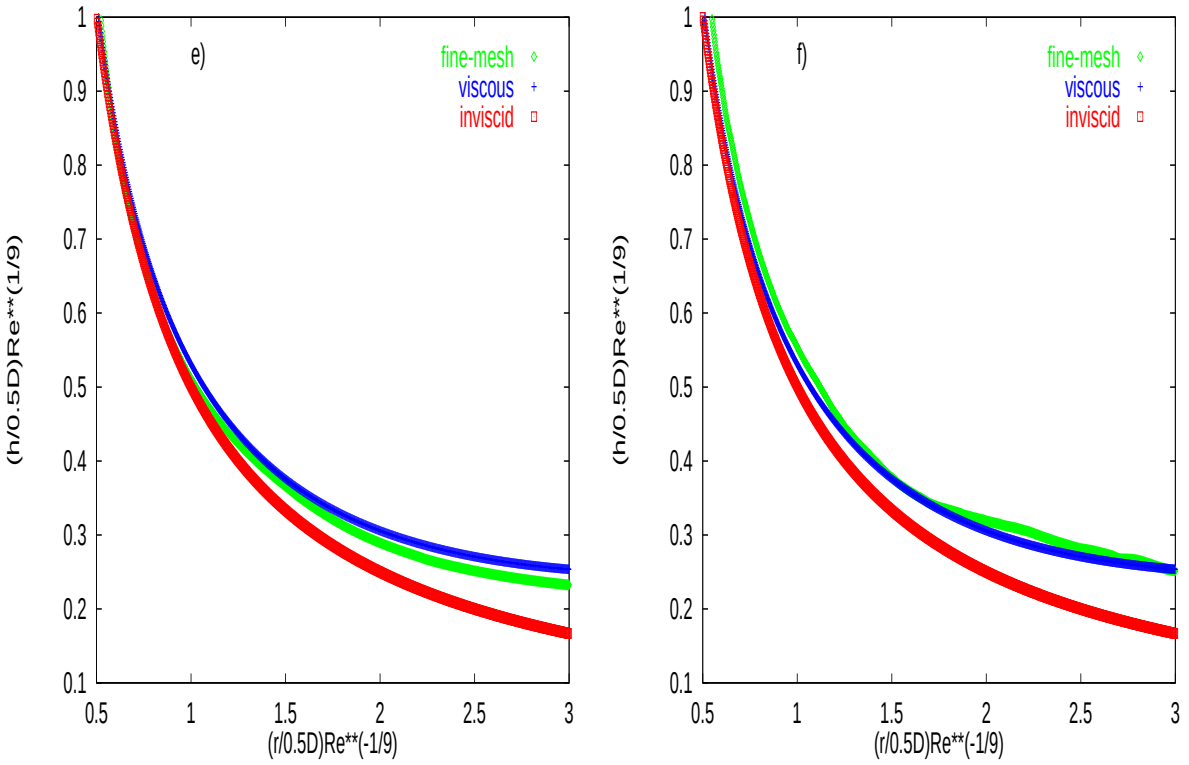

Figure 2: Continued

Hoffman, G., 1975, Improved Form of the Low Reynolds Number $\kappa - \varepsilon$ Turbulence Model, "The Physics of Fluids", Vol. 18, pp. 309–312.

Ladau, L. D. and Lifshitz, E. M., 1987, "Fluid Mechanics", Ed. Butterworth-Heinemann, 2^o Ed., Great Britain, Course of Theoretical Plysics V. 6.

Lauder, B. E. and Spalding, D. B., 1974, The Numerical Computation of Turbulent Flows, "International Journal for Numerical Methods in Fluids", Vol. 15, pp. 127–146.

Merci, B., Langhe, C. D., Vierendeels, J., and Dick, E., 2001, A Quasi-Realizable Cubic Low-Reynolds Eddy-Viscosity Turbulence Model with a New Dissipation Rate Equation, "Flow, Turbulence and Combustion", Vol. 66, pp. 133–157.

Norris, H. L. and Reynolds, W. C., 1975, Turbulent Channel Flow with a Moving Wavy Boundary, Stanford Univ. Dept. Mech. Eng.,TR TF-7.

Sondak, D. L. and Pletcher, R. H., 1995, Application of Wall Functions to Generalized Nonorthogonal Curvilinear Coordinate Systems, "AIAA Journal", Vol. 33, pp. 33–41.

Tomé, M. F., Castelo, A., Murakami, J., Cuminato, J. A., Minghim, R., Oliveira, C. F., N, M., and McKee, S., 2000, Numerical Simulation of Axisymmetric Free Surface Flows, "Journal of Computational Physics", Vol. 157, pp. 441–472.

Tomé, M. F. and McKee, S., 1994, GENSMAC: A Computational Marker-and-Cell Method for Free Surface Flows in General Domains, "Journal of Computational Physics", Vol. 33, pp. 171–186.

Varonos, A. and Bergeles, G., 1998, Development and Assessment of a Variable-Order Non-Oscillatory Scheme for Convection Term Discretization, "International Journal for Numerical Methods in Fluids", Vol. 26, pp. 1–16.

Watson, E. J., 1964, The Radial Spread of a Liquid Jet over a Horizontal Plane, "Journal of Fluid Mechanics", Vol. 20, pp. 481–499.

White, F. M., 1991, "Viscous Fluid Flow", Ed. McGraw-Hill, Inc., 2^o Ed., New York, USA.

Wilcox, D. C., 1988, Reassessment of the Scale-Determining Equation for Advanced Turbulence Models, "AIAA Journal", Vol. 26, pp. 1299–1310.

Yang, Z. and Shih, H., 1993, New Time Scale Based $\kappa - \varepsilon$ Model for Near-Wall Turbulence, "AIAA Journal", Vol. 7, pp. 1191–1198.